

## Transects by submarine of the East Greenland Polar Front

P. WADHAMS\*, A. E. GILL† and P. F. LINDEN†

(Received 2 January 1979; in revised form 2 May 1979; accepted 5 August 1979)

**Abstract**—Seven transects of the East Greenland portion of the Polar Front were made by HM nuclear submarine *Sovereign* in October 1976. The transects, between 71 and 81°N, comprise continuous horizontal sound velocity profiles at depths of between 67 and 125 m, accompanied by inverted sonar profiles of the ice canopy overhead. Features of the sound velocity profiles include steep thermal fronts; high-frequency structure, possibly due to internal waves and found mainly in the Front; and warm water patches within the zone of Polar Water, probably due to eddies. Once the submarine passed through the Front twice by diving, which enables an estimate of its slope to be made. The nature of the features that suggest internal waves and eddies is considered, and an analysis is made of the extent to which a warm surface eddy can cause the ice cover to melt if assisted by wave action. A laboratory experiment is also described in which the East Greenland Current was modelled by releasing a cylinder of salt water placed in the centre of a rotating circular tank of freshwater, with a radial barrier simulating Greenland. A current was obtained along the eastern side of the barrier, reproducing many of the qualitative features of the East Greenland Current.

### INTRODUCTION

THE COLD, fresh Polar Water that occupies the upper layers of the Arctic Ocean flows out along the east coast of Greenland, forming the upper part of the East Greenland Current. The eastern edge of this Polar Water, where it is found off East Greenland, can be referred to as the East Greenland portion of the Polar Front. Hydrographic sections across the East Greenland Current were made as long ago as 1905 and 1906 (KILIERICH, 1945), and this and more recent work were discussed by AAGAARD and COACHMAN (1968). The sections show that the Polar Water occupies a wedge-shaped region bounded by the surface above, a sloping interface below, and the Greenland coast on the side. The interface is at a depth of 200 m or more where it strikes bottom on the shelf and slopes upward to the east to reach the surface some 200 km away, so that its average slope is roughly 1 in 1000.

In October 1976, transects of this sloping interface were made by submarine. Continuous measurements of sound velocity were made, thus giving an indication of the sharpness of the front and of the horizontal scales in the sound-velocity structure on either side of the front. In addition, continuous measurements of ice draft were made using upward-looking sonar, so the relationship of the sound velocity structure to the ice field above could be seen.

### THE OBSERVATIONS

The sound velocity profiles were obtained during a cruise to the Arctic Ocean by HM nuclear submarine *Sovereign* (WADHAMS, 1977). The main purpose of the cruise was to

---

\* Scott Polar Research Institute, University of Cambridge, Cambridge CB2 1ER, U.K.

† Department of Applied Mathematics and Theoretical Physics, University of Cambridge, Cambridge CB3 9EW, U.K.

obtain corresponding profiles of the bottom and top surfaces of the ice cover using a submarine and aircraft operating in concert (WADHAMS, 1979), but during the initial and final stages of the cruise *Sovereign* made many independent transects of the Polar Front between 71 and 81°N (Fig. 1). She was equipped with a velocimeter that records the local sound velocity by sending pulses round a short quadrilateral path and measuring the time of transit; the meter fed a Servoscribe chart recorder that provided a continuous record of sound velocity. The accompanying ice profile was obtained by an upward-looking echo sounder mounted on the bow; the transducer had beam widths of 17° fore-and-aft and 5° athwartships, and fed a Kelvin Hughes MS45 recorder operating at 45 kHz. *Sovereign* was also equipped with a projector for expendable bathythermographs (XBTs), a limited number of which were launched during the cruise. Position fixing was done by using a Ship's Inertial Navigation System (SINS).

The records obtained are shown in Figs 2 to 8. The ice draft profiles display 'mean' and 'extreme' ice drafts. The mean value is the mean draft of undeformed floes; the extreme value is the maximum draft of pressure ridges which occur with reasonable frequency. Isolated floes in open water areas are shown by single vertical bars. Time marks are given every half hour on account of minor variations in the speed of the Servoscribe recorder.

The sound velocity  $c$  in the area studied is a function mainly of temperature  $T$  and depends only weakly on salinity  $S$  and depth  $D$ . For instance, a combination of formulae on p. 105 of TOLSTOY and CLAY (1966) gives

$$c = 1449.2 + 4.623T - 0.0546T^2 + 1.391(S - 35) + D/61 \quad (1)$$

where  $c$  is in  $\text{m s}^{-1}$ ,  $T$  in °C,  $S$  in parts per thousand, and  $D$  in metres. The temperature-salinity sections in the area suggest that the low sound velocities are associated with water having a temperature near  $-1.5^\circ\text{C}$  and a salinity near  $34\text{‰}$ . At a depth of 85 m the above formula then gives  $c = 1442$ . The high velocities, on the other hand, are probably associated with water having a salinity near  $35\text{‰}$  and a temperature of about  $4^\circ\text{C}$ , giving  $c = 1468$ . Thus, taking into account the weak salinity effect, it seems reasonable to assume that a change of sound velocity of  $4.7 \text{ m s}^{-1}$  roughly corresponds to a change of temperature of  $1^\circ\text{C}$ .

Figures 2 to 6 show transects at latitudes 79 to 81°N. The ice in most of these transects extends several tens of kilometres beyond the first signs of warm water at the depth of observation. However, it should be borne in mind that the Front is a sloping surface. If the slope is 1 in 1000, then the Front at a depth  $D$  m would be displaced at a distance  $D$  km from the surface expression of the Front. The slope of the Front may well be greater than 1 in 1000 near its edge, so the ice edge may not be displaced very far from the surface front at these high latitudes. Figure 2 shows when the submarine passed through the front at two different depths, giving a lower limit for the slope of the Front at that latitude of 1 in 1200.

The transects show signs of eddy activity along the Front as patches of warm water (warm eddies) are sometimes found well inside the Front. This is particularly apparent in the transect of 29 to 30 October (Fig. 5). One of the warm eddies had a considerably thinner ice cover above it, but this may be an effect of advection rather than melting, as it is quite likely that the warm patch did not extend all the way to the surface. The eddies may well be similar to those seen in Landsat images of the ice edge (VINJE, 1979), although a one-dimensional transect does not provide sufficient information for resolution of structure or scale.

The transects made further south (Figs. 7 and 8) are rather different. The one near 76°N

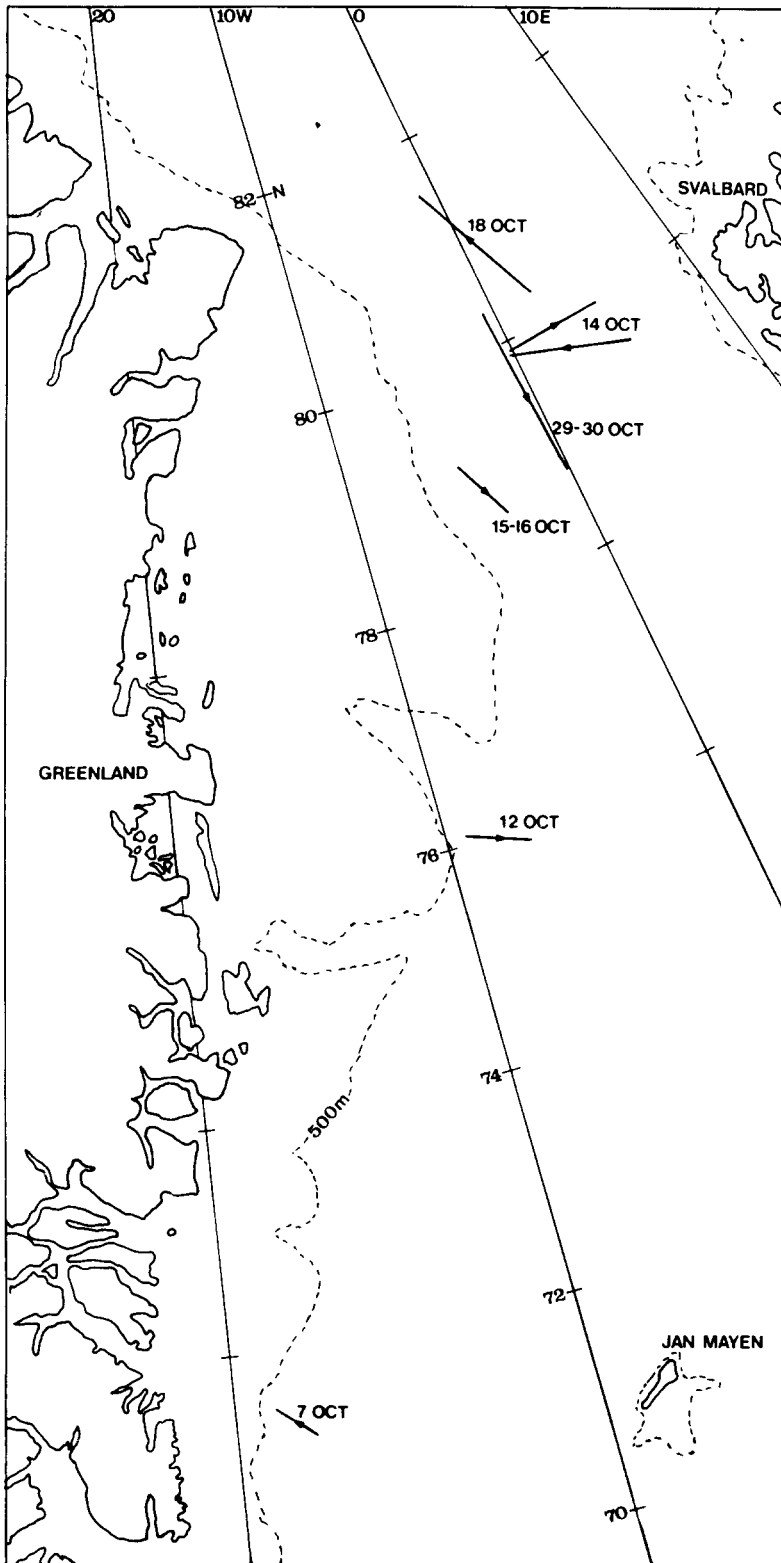


Fig. 1. Map showing positions of transects across East Greenland Polar Front.

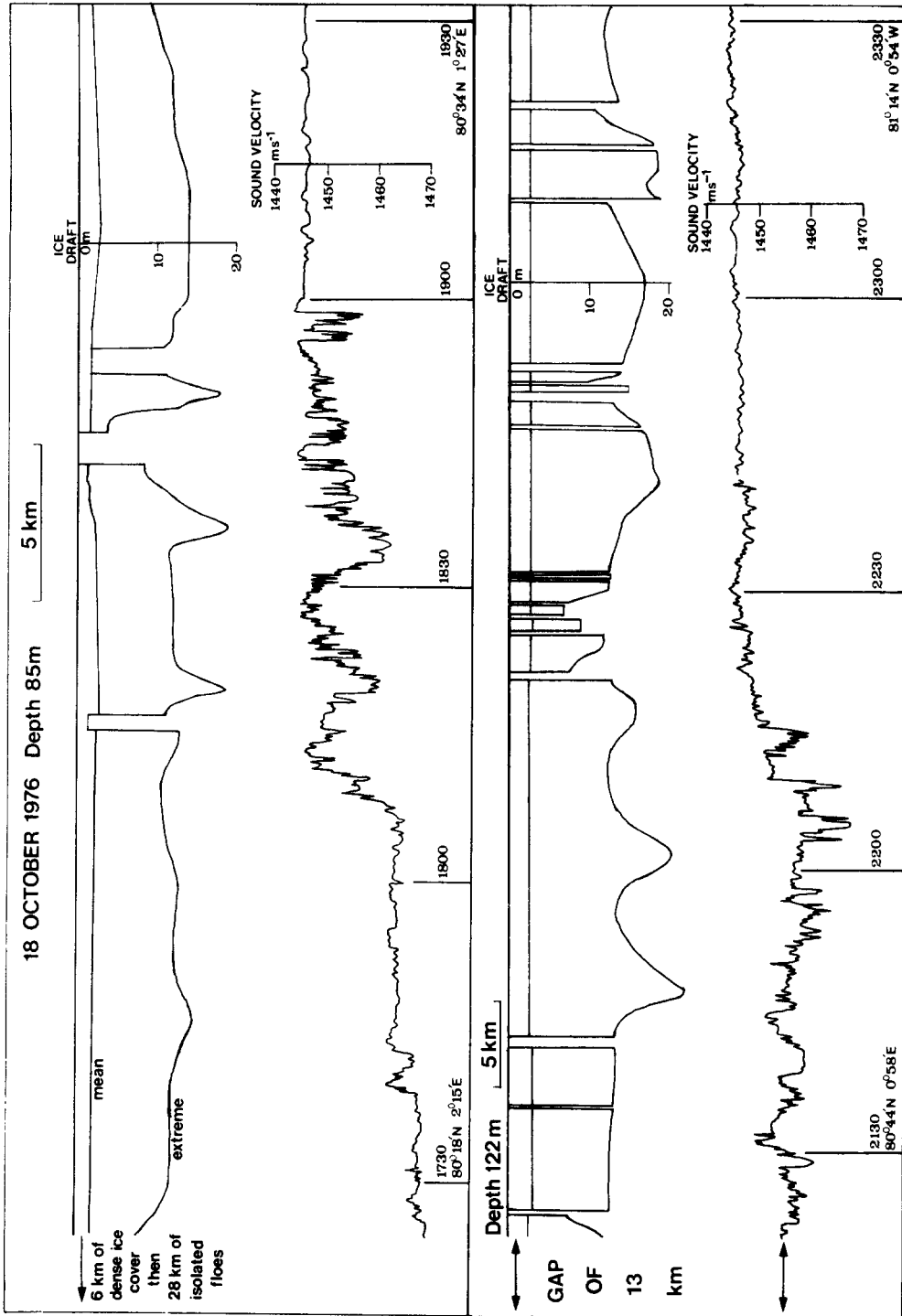


Fig. 2. Two sound velocity profiles from passage into ice at  $80^{\circ}$  to  $81^{\circ}N$ , 18 October 1976. At a depth of 85 m (top profile) the Polar Front begins some 20 km inside the ice edge, neglecting a belt of isolated floes lying outside the main edge. At  $19:30$  GMT the submarine dived deeper and continued on her course at a depth of 122 m. At this depth (bottom profile) a front with a smaller and gentler velocity step was encountered 44 km further into the ice than the earlier front. This implies that the Polar Front slopes inwards towards the cold water zone with increasing depth, and that by diving deeper the submarine crossed the Front twice. If the direction of greatest slope lies parallel to the submarine's course ( $333^{\circ}$  true), the slope of the front is 1 in 1200; otherwise this is a lower limit.

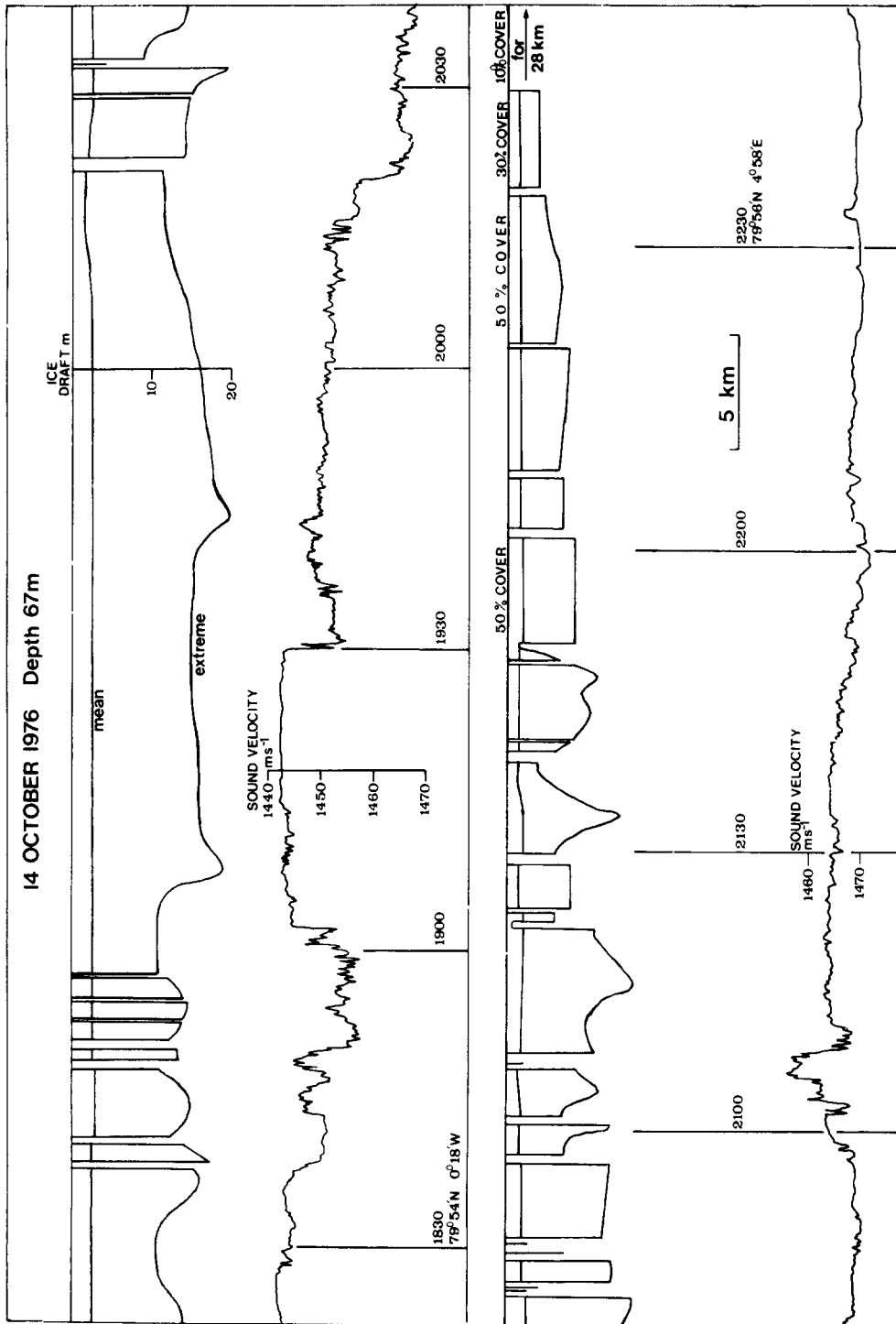


Fig. 3. Sound velocity profile from passage out of the ice at 80°N, 14 October 1976. Course of submarine was due east. There is considerable structure in the profile, with sudden transitions of order  $10 \text{ m s}^{-1}$ , but the warm ( $1470 \text{ m s}^{-1}$ ) water begins at 20 : 20 GMT, 38 km before the ice breaks up into a 50% cover and 91 km before completely open water is reached. Note the cold water patch at 21 : 10 GMT.

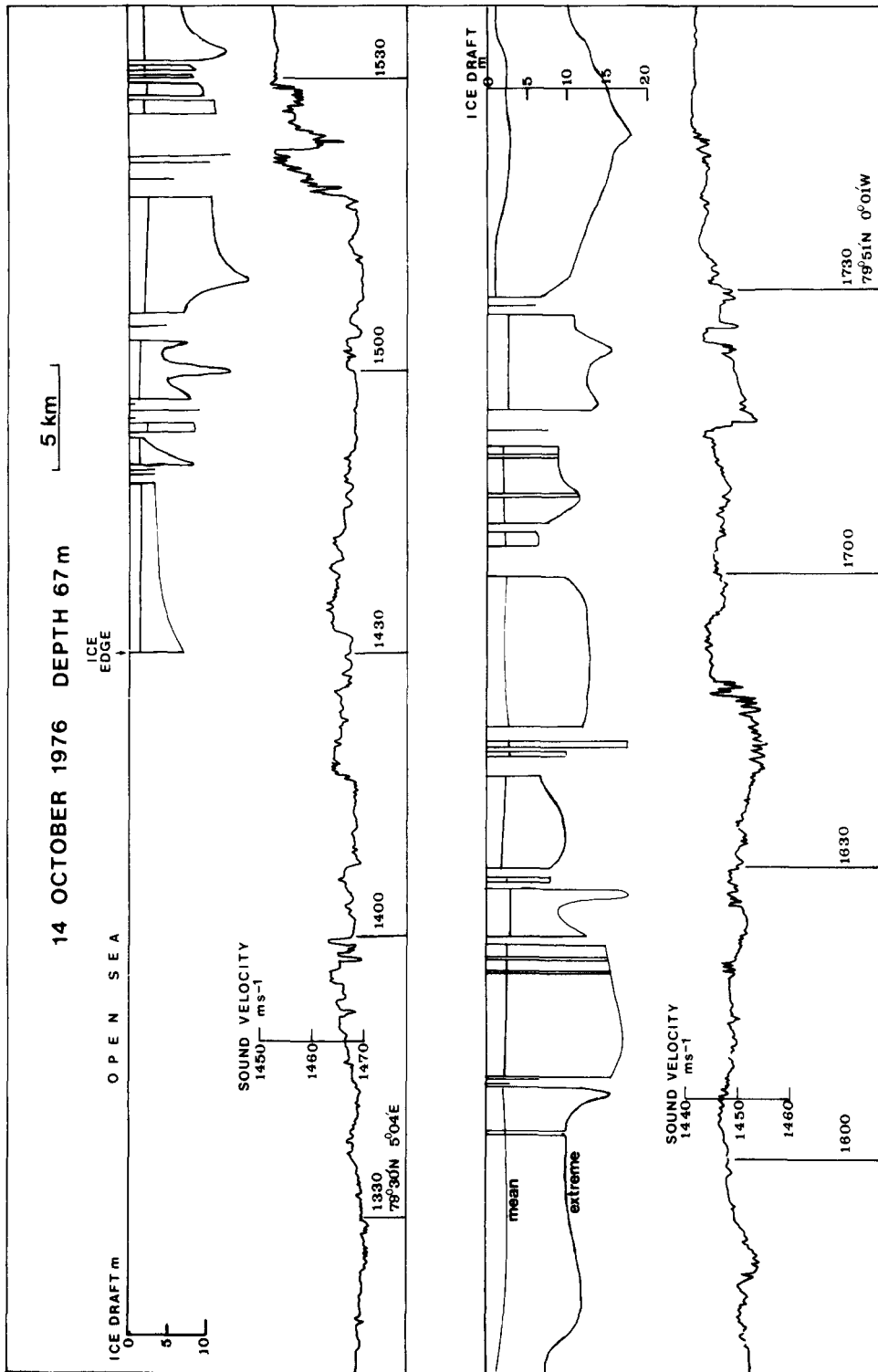


Fig. 4. Sound velocity profile from passage into ice at 79°40'N, 14 October 1976, observed just before the profile in Fig. 3. Although the profile shows considerable structure at and outside the ice edge, the sharp fall to cold water does not occur until 22 km inside the ice edge.

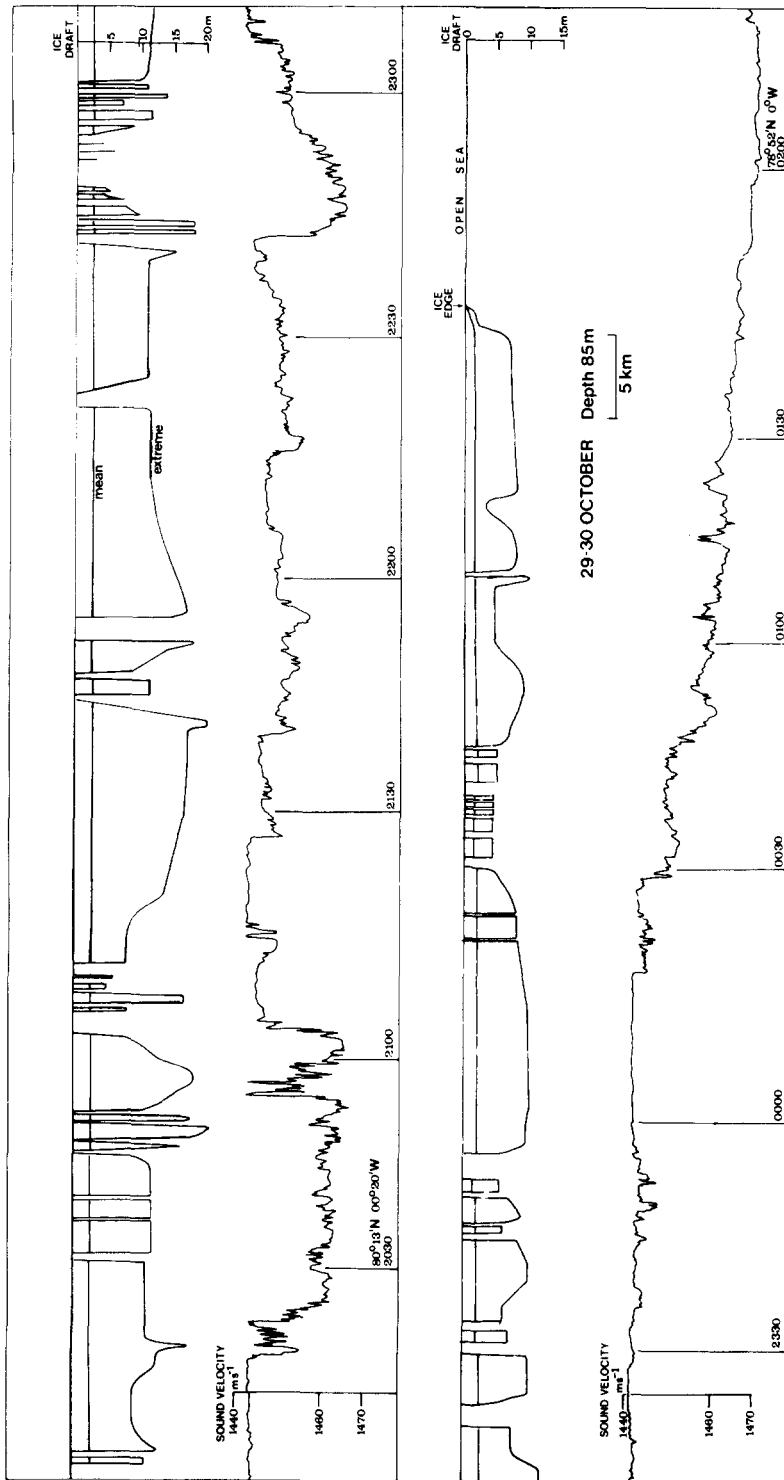


Fig. 5. Sound velocity profile obtained during passage out of ice, 29-30 October 1976. There are two stretches of warm water within the ice-covered zone, at 20:15 to 21:05 GMT and 22:45 to 23:10 GMT, the second of which correlates well with a region of attenuated ice cover. The widths of the warm intervals are 20 and 12 km, respectively, and they have very sharp boundaries; the transition to warm water near the outer ice edge is gentler.

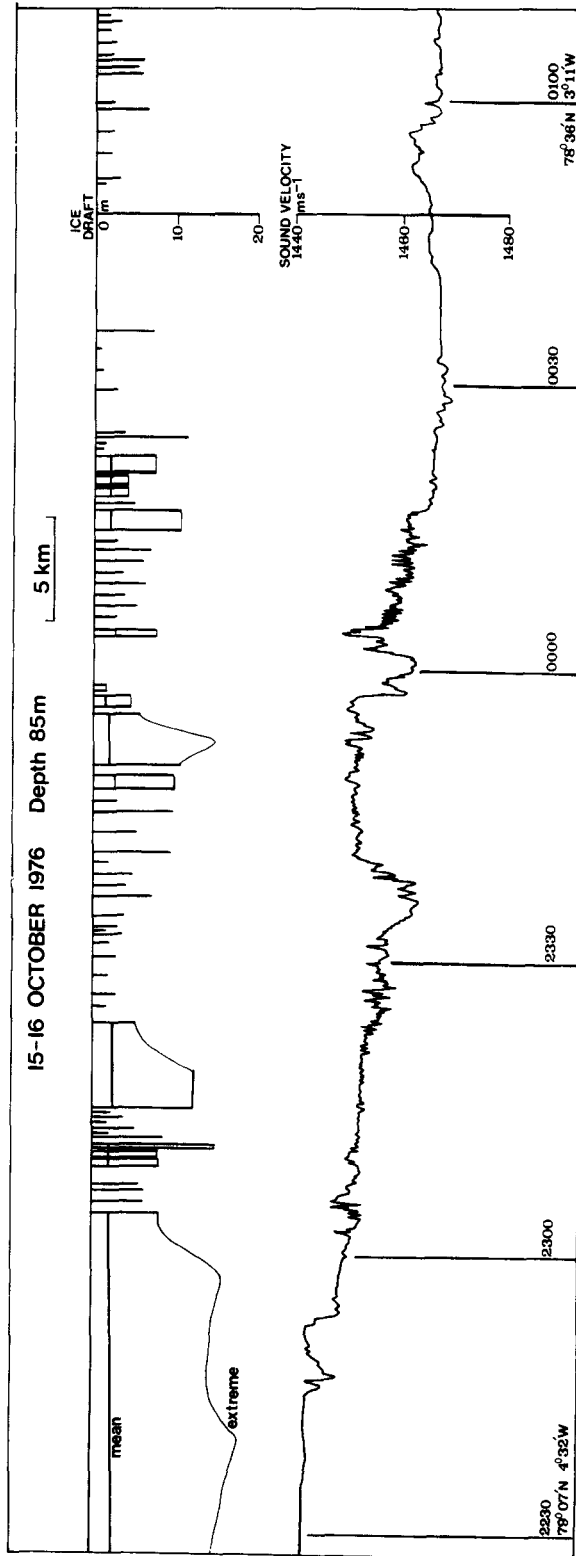


Fig. 6. Sound velocity profile from passage out of ice at 79°N, 15–16 October 1976. The ice edge is diffuse, showing a steady change from a continuous cover to isolated floes. The position of the Polar Front at 85 m corresponds roughly with that of the ice edge. Note the high-frequency structure in the sound velocity profile at the front, compared with the steady sound velocity beyond the front in the cold and warm water zones.

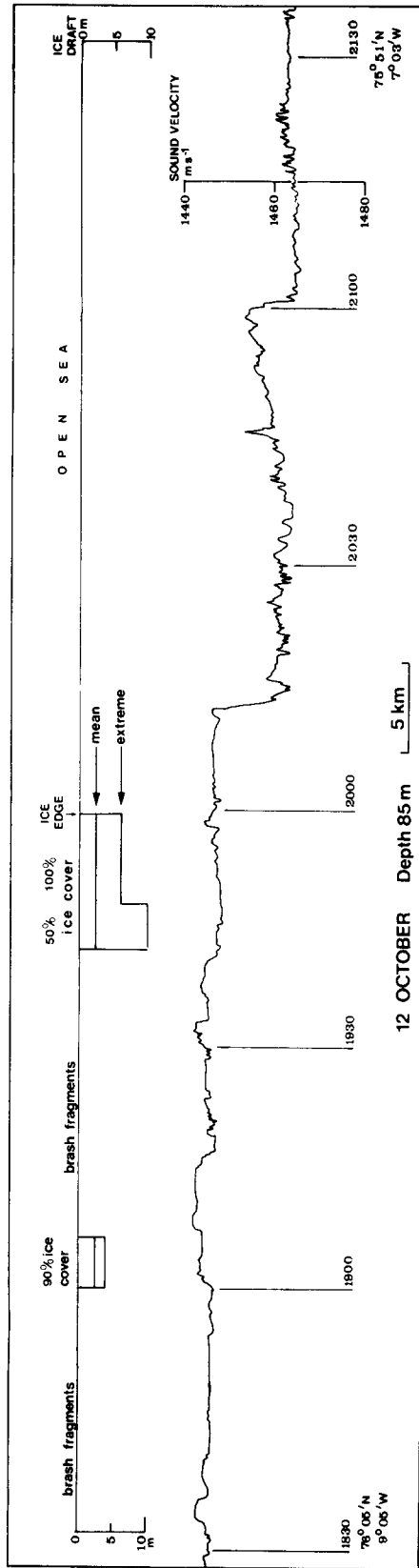


Fig. 7. Sound velocity profile obtained during passage out of East Greenland pack ice at  $76^{\circ}N$ , 12 October 1976. Note sharp transition to warm water, displaced by about 6 km from position of ice edge.

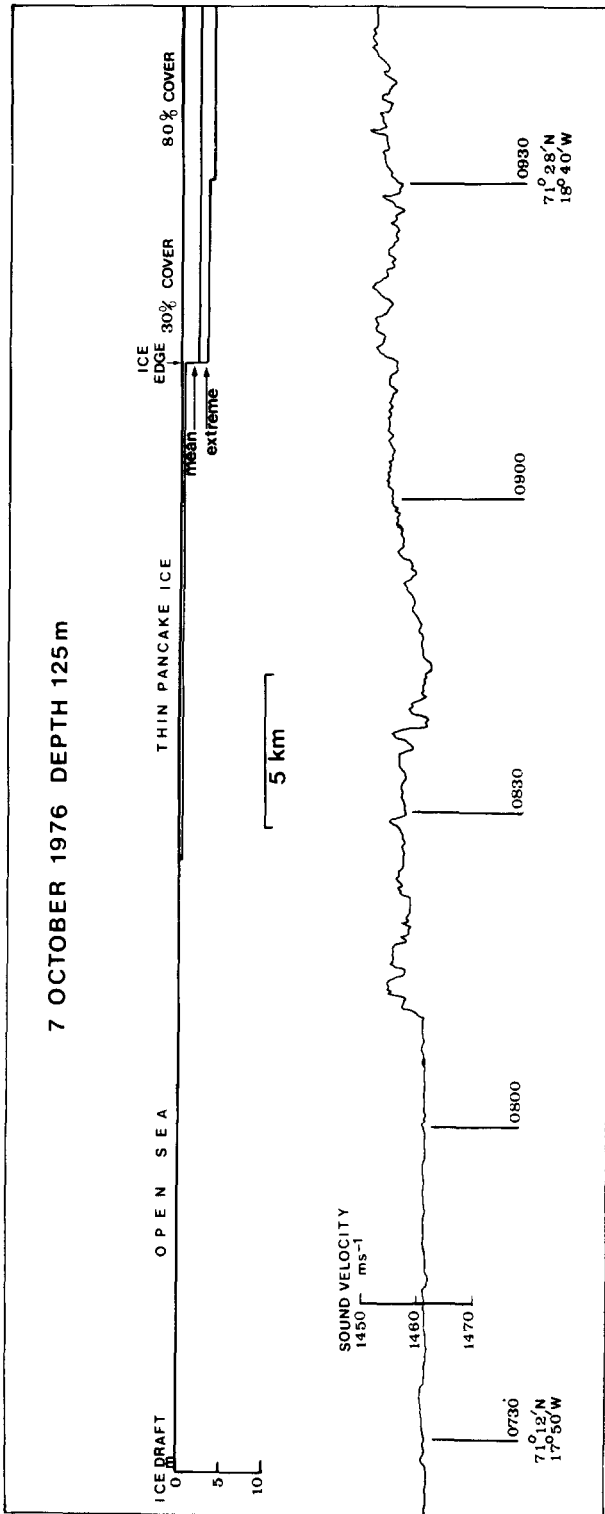


Fig. 8. Sound velocity profile from passage into East Greenland ice at latitude of Jan Mayen, 7 October 1976. At a depth of 125 m colder water begins 21 km outside the 'ice edge', defined as the first point at which floes were seen. In this case there are a further 6 km of scattered floes before the denser 80% cover begins.

(Fig. 7) shows a sharp thermal front about 6 km seaward of the ice edge, and the surface front was probably several tens of kilometres further seaward. It would appear that melting of ice had taken place and it is also possible that wind effects could have moved the ice relative to the front. The transect of 7 October (Fig. 8) shows only a weak front, which appears to start well seaward of the ice edge.

#### THE LARGE-SCALE FLOW

To understand the ice distributions, some idea of the large scale flow patterns in the area is required. The water found above and west of the Front comes from the Arctic Ocean and is less dense, despite being very cold, because of its low salinity. Water with similar properties occupies all of the upper part of the Arctic, and it might be expected to flow out between Greenland and Norway under the influence of gravity. But why should it flow only in a thin stream against the coast of Greenland? An experiment was carried out to examine this question.

##### *The experiment*

The Polar Water was modelled by a cylinder of salt solution placed in the centre of a circular tank 91 cm in diameter filled to a depth of 13 cm with freshwater. The salt solution was held in place by containing it within a bottomless perspex cylinder 15 cm in diameter resting on the bottom of the tank. The density difference  $\Delta\rho$  between the salt solution and the fresh water was  $\Delta\rho/\rho = 0.038$ . We can usefully consider three cases:

(a) If the tank is not rotating, then once the cylinder is lifted out the dense fluid slumps down and spreads out radially along the bottom of the tank. This motion is driven by the density difference and takes the familiar form of a gravity current. Here we are modelling the fresh Polar Water by the salt solution, the only difference being that in the laboratory simulation the current flows along the bottom rather than along the surface. This has no significant dynamical consequences.

(b) If the tank is rotating, and the fluid is initially in solid body rotation, then the dense fluid slumps down once the cylinder is removed but the radial spread is inhibited by the rotation. SAUNDERS (1973) studied this situation in some detail and found that, provided the density difference was large enough, the dense fluid remained coherent and axisymmetric. However, if the density difference was small the dense fluid broke up into a number of eddies, produced by baroclinic instability. The relevant non-dimensional parameter determining the stability of the dense fluid is

$$\Theta = \frac{g'H}{R_0^2 f_r^2}, \quad (2)$$

where  $g' = g\Delta\rho/\rho$ ,  $H$  is the fluid depth,  $R_0$  the initial radius of the dense fluid, and  $f_r$  is twice the angular velocity of the fluid. Saunders found that the dense fluid mass was stable provided  $\Theta \gtrsim 1.5$ .

The slumping of the dense fluid compresses vertical vortex lines in the dense fluid producing anticyclonic motion. The fluid that moves in over the top has cyclonic motion induced in it. After the initial slumping of the fluid it achieves geostrophic balance with the horizontal density gradients balanced by the vertical shear (the thermal wind). In the absence of dissipation and diffusion this new state would be maintained indefinitely. In

practice, however, frictional forces would eventually spin the fluid up allowing it to spread still further, but this occurs over a much larger time scale.

(c) The third situation, and the experiment carried out here, concerns the influence of a radial barrier on this geostrophic adjustment. In the configuration already described a radial barrier was introduced. The barrier consisted of a vertical sheet of perspex 35 cm long occupying the full depth of the tank. It was attached to the outer wall of the tank and came to within 3 cm of the bottomless cylinder. The tank was rotated at  $1.1 \text{ rad s}^{-1}$ , giving  $\Theta = 1.7$ , and the whole system was spun up until it was in solid body rotation.

Figure 9 shows a plan view of the experiment approximately 3 s after the cylinder was removed. The dense water, which was dyed and so shows up dark on the photograph, has slumped to a radius of 12 cm, as in the case when the barrier was absent. However, there is now a current travelling along one side of the radial barrier. The speed  $u$  of the front of this current is approximately  $10 \text{ cm s}^{-1}$ , and it has a width of about 3 cm. The depth  $d$  of this current was approximately 1 cm, giving a Froude number of advance  $Fr = u (g'd)^{-1/2} = 1.6$ . The sense of rotation is that of the northern hemisphere (anticlockwise on Fig. 9) and so the current flows along the eastern side of the boundary.

The presence of the current is readily explained. As there is no motion normal to the boundary, there can be no Coriolis acceleration parallel to it. Consequently the rotational constraint is lost and the buoyancy forces drive a current as in the non-rotating system. Gravity currents in non-rotating systems travel with Froude numbers around unity (see BRITTER and SIMPSON, 1978). The width of the current is set by the internal Rossby radius  $(g'd)^{1/2}/f_r$ , which is 2.8 cm for this experiment, in good agreement with the observed width. The current is found only on the eastern side of the barrier as the flow along the boundary is in geostrophic equilibrium with the pressure gradient normal to the boundary. In the northern hemisphere these currents move with the coast on the right, whether they are surface or bottom currents.

As a result of this experiment, we conclude that the East Greenland Current is basically a result of buoyancy forces acting as described in the experiment. Wind effects strongly influence the strength of the current, particularly in the south (AAGAARD, 1970), but they do not explain the distribution of properties and the existence of the Front.

Since the Arctic is ice-covered, the stream of fresh water that flows from the Arctic carries ice with it. This is the main reason ice is found off northeast Greenland and also why ice tends to be found in water derived from the Arctic but not in the warmer waters of the Greenland Sea, which have a different origin. Observations of ice drift (VINJE, 1977a) indicate that the ice takes about a month to move from latitude  $80^\circ$  (where the transects shown in Figs 2–6 were made) to latitude  $76^\circ$  (transect shown in Fig. 7) and another month to reach latitude  $72^\circ$  (transect shown in Fig. 8). During these weeks a relatively small wind drift of the ice with respect to the water could explain the observed lateral displacement of the ice edge relative to the thermal front.

The position of the ice front can also be affected by melting, the rate of which can be considerably greater near the ice front because of wave action. This effect is estimated in the next section.

#### WAVE-INDUCED MELTING OF ICE

The two southern transects (Figs 7 and 8) show that the ice edge lay well to the west of the probable position of the thermal front at the surface. There are many reasons for this

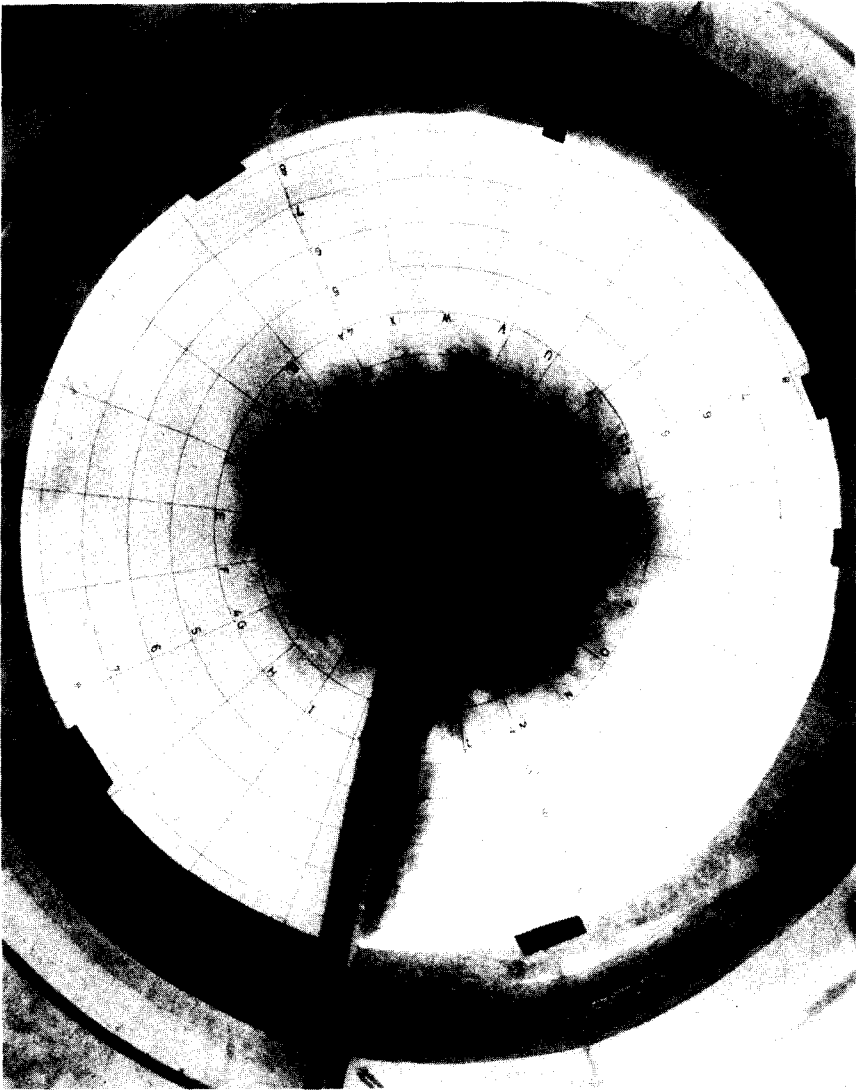


Fig. 9. The experiment. A plan view of the flow taken approximately 3 s after the bottomless cylinder was removed. The dyed dense water is constrained near the centre of the tank except near the radial barrier where it flows radially with the boundary on its right. The sense of rotation is anticlockwise and the concentric circles on the bottom of the tank have incremental radii of 4 cm.

retreat of the ice. To reach 71°N by October the ice had undergone a two-month passage down the east Greenland coast during August and September when positive air temperatures and absorption of solar radiation cause surface melting, and where any divergence of the ice will lead to rapid absorption of heat in the newly-created open water areas with consequent lateral melting of floe edges. Bottom melting also occurs when the water temperature is above the melting point, due to turbulent heat flux from the water, which depends on the relative velocity of the ice and surface water. This is also the basis for wave-induced melting that acts preferentially at or near the ice front and causes retreat of the ice front as opposed to uniform melting throughout the ice field.

The swell component of a sea can penetrate for tens of kilometres into an ice cover, and WADHAMS (1978) has shown that the incoming swell suffers an exponential decay with typical values for the amplitude attenuation rate of  $0.4$  to  $0.7 \times 10^{-4} \text{ m}^{-1}$  for a 12 to 13-s swell and  $1.2 \times 10^{-4} \text{ m}^{-1}$  for a 10 to 11-s swell. The swell produces an oscillating, horizontal velocity component in the water relative to the ice bottom that permits turbulent diffusion of heat into the ice provided the water is warmer than the ice.

According to CSANADY (1972) the heat flux into a horizontal boundary surface on account of a steady shear current  $V$  of water at a temperature  $\Delta T$  above that of the surface is

$$H_v = c_H \rho_w c_w \Delta T V, \quad (3)$$

where  $\rho_w$  is the water density,  $c_w$  is its specific heat, and  $c_H$  is a dimensionless parameter estimated by GILL (1973) as being of the order of  $3 \times 10^{-3}$  for the bottoms of Antarctic ice shelves. Gill also estimated that  $c_H$  must be reduced by 40% for a factor of 10 reduction in the roughness length of the interface. It is likely that floe bottoms have a lower roughness length than shelf bottoms; further, it is likely that the turbulence in an oscillating flow is less well developed than in a steady flow, necessitating a further reduction in  $c_H$ . A suggested value to use is thus about  $10^{-3}$ , although this is based on guesswork.

The melt rate predicted by (3) is  $(H_v/\rho_i L)$ , where  $\rho_i$  is the density of the ice and  $L$  is its latent heat of fusion. We assume that the temperature of the ice bottom is the melting point.

The mean horizontal velocity at zero depth due to a wave of amplitude  $A$  and angular frequency  $\omega$  is  $(2A\omega/\pi)$ ; if the wave has amplitude  $A$  at the ice edge and penetrates a distance  $s$  into the ice with an amplitude attenuation rate  $\alpha$ , then we have

$$V = \left( \frac{2A\omega}{\pi} \right) \exp(-\alpha s) + V_0, \quad (4)$$

assuming that the floes have no surge response to the wave and that the ice draft is small compared to a wavelength. Very close to the ice edge, where the average floe is small, the surge response is considerable so that (4) is an over-estimate of  $V$ .  $V_0$  is the steady shear current (due to wind-induced relative drift) in the absence of waves.

Putting  $c_w = 4.0 \text{ kJ kg}^{-1} \text{ }^\circ\text{C}^{-1}$ ,  $L = 335 \text{ kJ kg}^{-1}$ , and  $\rho_i/\rho_w = 0.9$ , we obtain

$$\text{Melt rate in } \text{m s}^{-1} = 8.4 \times 10^{-3} c_H \Delta T \{A\omega \exp(-\alpha s) + V_0\}. \quad (5)$$

We can now estimate the time required to melt a floe 3 m thick, typical of East Greenland sea ice. WADHAMS (1978) showed that  $\alpha$  increases approximately as  $\omega^2$ , so that short-period waves have no influence except at the extreme ice edge. In Fig. 10 we consider two wave periods, 10 and 13 s (a typical range of spectral peaks for the East Greenland coast), putting  $\alpha = 1.2$  and  $0.7 \times 10^{-4} \text{ m}^{-1}$ , respectively, and plot the melting time at different distances

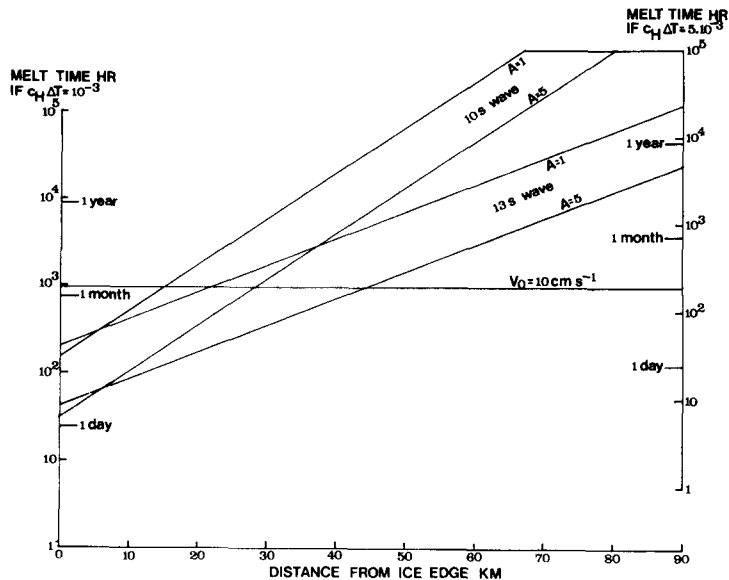


Fig. 10. The time taken to melt a 3-m floe by wave action estimated for 10-s and 13-s waves. For comparison the melting time due to a steady current of  $10 \text{ cm s}^{-1}$  is also shown.

inside the ice edge for two values of  $c_H \Delta T$  ( $10^{-3}$  and  $5 \times 10^{-3}$ ) and of  $A$  (1 and 5 m). For comparison we also plot the melt time for  $V_0 = 10 \text{ cm s}^{-1}$ , typical of wind induced drift. The conclusions that can be drawn are:

(i) At the ice edge itself wave-induced melting is very effective. The waves with 5-m amplitude will melt a floe in 1 to 2 days and in 6 to 8 days with 1-m amplitude even when  $c_H \Delta T = 10^{-3}$  (i.e., approximately a  $1^\circ\text{C}$  temperature difference). With  $c_H \Delta T = 5 \times 10^{-3}$  (a  $5^\circ\text{C}$  temperature difference between ice and water) the times are only 6 to 8 h (5-m waves) and 1 to 2 days (1-m amplitude). It is clear that wave-induced bottom melting is constantly in progress at the ice edge, eating away at the floes and eroding the edge westward. In winter this process is opposed by freezing, but it may account for the frequent observations that floes near the ice margin have a net component of drift towards the margin (e.g., VINJE, 1977b).

(ii) Beyond 6-km penetration the 13-s wave is more effective than a 10-s wave of the same amplitude, and the difference becomes steadily larger. Thus only the longer swells are effective at deep penetrations.

(iii) Up to a penetration of 22 km ( $A = 1$ ) or 44 km ( $A = 5$ ), a 13-s swell is more effective at melting the ice than a  $10 \text{ cm s}^{-1}$  shear current. Thus up to this penetration wave-induced melting is the dominant mode of bottom melting, while beyond this penetration it is a small effect which adds to the melt rate due to wind-induced shear currents.

(iv) At a penetration of 75 km (the position of the outermost warm patch in Fig. 5) a 13-s swell of 5-m amplitude requires 11 months to melt a floe if  $c_H \Delta T = 10^{-3}$  and 2 months if  $c_H \Delta T = 5 \times 10^{-3}$ . The corresponding times for a  $10 \text{ cm s}^{-1}$  current are 41 and 8 days. Thus, assuming that the warm patch in Fig. 5 extends directly to the surface (which is not necessarily so), the diminished ice cover seen above it is more likely to be caused by shear

current melting than by wave melting. It is also possible that the eddy has caused a divergence in the surface drift field or that open water was entrained from the Greenland Sea at the time the eddy was formed.

#### SMALL SCALE FEATURES

The sound velocity profiles in Figs 2 to 8 show considerable small-scale structure. The transition from the cold, fresh Polar Water to the warmer, more saline, Greenland Sea water is sharp, usually only 1 km or so in horizontal extent. Small scale features are also observed in the profiles, showing structure with horizontal scales of the order of a hundred metres or so. The amplitudes of these features are much greater than those observed well away from the Front, showing that they are much larger than the noise level of the instrument.

There are some differences in the small scale structure between the cold and the warmer regions. The amplitude of the fluctuations is generally larger in the warm patches than in the colder water. This can be seen clearly from the sound velocity profiles. Spectra of the 12 October transect (Fig. 7) show considerably more energy at smaller scales ( $< 300$  m) in the warm than in the cold water.

There are two likely causes of these small-scale features. One is that they are produced by isopycnal distortion due to internal waves. For a given wave amplitude the magnitude of the temperature fluctuations will be proportional to the temperature gradient. This implies that the fluctuations will be largest where the temperature gradients are largest, i.e., near the front between the Polar Water and the warmer Greenland Sea water. The decrease in magnitude of the fluctuations with distance from the front can be clearly seen, for instance in Fig. 5. The same argument also applies to the warm patches observed in the Polar Water, where large fluctuations were observed (see Fig. 5).

A second possible cause of the small-scale structures is double diffusive convection, as there is warm, saline water adjacent to colder and fresher water, both at the Front and in the warm patches in the East Greenland Current. Laboratory experiments (TURNER and CHEN, 1974; LINDEN and WEBER, 1977) have shown that in this situation interleaving tongues of the two water masses intrude into each other. Similar intrusions can be seen on Fig. 11, which shows a temperature–depth profile taken using an XBT (expendable bathythermograph) at  $78^{\circ}50'N$ ,  $02^{\circ}08'W$  on 15 October at 15:45 GMT while the submarine was surfaced in an open icefield. The uppermost 15 m of the profile were lost because the XBT was launched from within the submarine. The position is close to that of the sound velocity profile shown in Fig. 6, and it is clear that the submarine is within the Polar Water, with the Polar Front occurring at 150 to 180 m. This profile shows two warm features, at 40 and 100 m, which must have high salinity otherwise they would be statically unstable. The profile also shows steep structures in the temperature inversion above the Polar Front, characteristic of double-diffusive convection.

The observed small-scale features are probably a result of internal waves and double diffusion acting together.

#### EDDIES

The warm patches well inside the Front and the evidence from Landsat imagery point to the existence of eddies along the Front, indicating a possible instability of the Front. In this

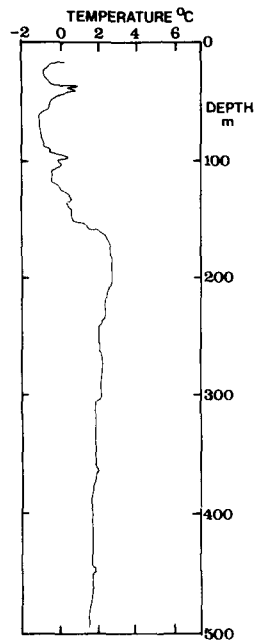


Fig. 11. XBT profile of temperature against depth taken at 15 : 45 GMT on 15 October 1976.

connection, a study of boundary current instabilities by JONES (1977) is relevant. He considered a two-layer system where the upper layer forms a wedge of constant slope adjacent to a vertical boundary in an ocean of uniform depth  $H$ . If  $L$  is the width of the wedge of less dense water and  $D$  is its depth at the vertical wall (so that the interfacial slope is  $D/L$ ), with  $D \ll H$ , Jones found that the criterion for instability is approximately given by  $L > L_{\text{crit}}$ , where

$$L_{\text{crit}} = g'^{\frac{1}{2}}(HD)^{\frac{1}{4}}/f. \quad (6)$$

Here  $f$  is the Coriolis parameter and  $g'$  is the reduced gravity defined as in equation (2).  $L_{\text{crit}}$  is about 25 km for the East Greenland Current. The Current is wider than  $L_{\text{crit}}$  at all latitudes, suggesting that the East Greenland Polar Front is unstable along its whole length. It seems reasonable to conclude, therefore, that the observed eddies are the result of instability of the front.

Figure 12, reproduced by courtesy of T. E. Vinje, is a Landsat image (E2473-13120) obtained on 9 May 1976 showing an ice feature at the edge of the East Greenland Current which is clearly an eddy. The centre of the eddy is at about  $79^{\circ}30'N$ ,  $3^{\circ}E$  and its diameter is about 60 km. VINJE (1979) also found that a Nimbus-6 satellite-tracked data buoy became trapped in the same eddy in July 1976, enabling its surface temperature structure to be contoured. At that time the eddy's centre was at about  $80^{\circ}00'N$ ,  $2^{\circ}E$ . Vinje suggested that this may be a semi-permanent bottom-steered eddy, because charts of the area show a circular depression (the Molloy Deep) about 2000 m deeper than the surrounding ocean bottom, centred at  $79^{\circ}15'N$ ,  $3^{\circ}E$  and of diameter 60 km. Evidence in support of this hypothesis comes from earlier observations of a feature near this position, ranging from

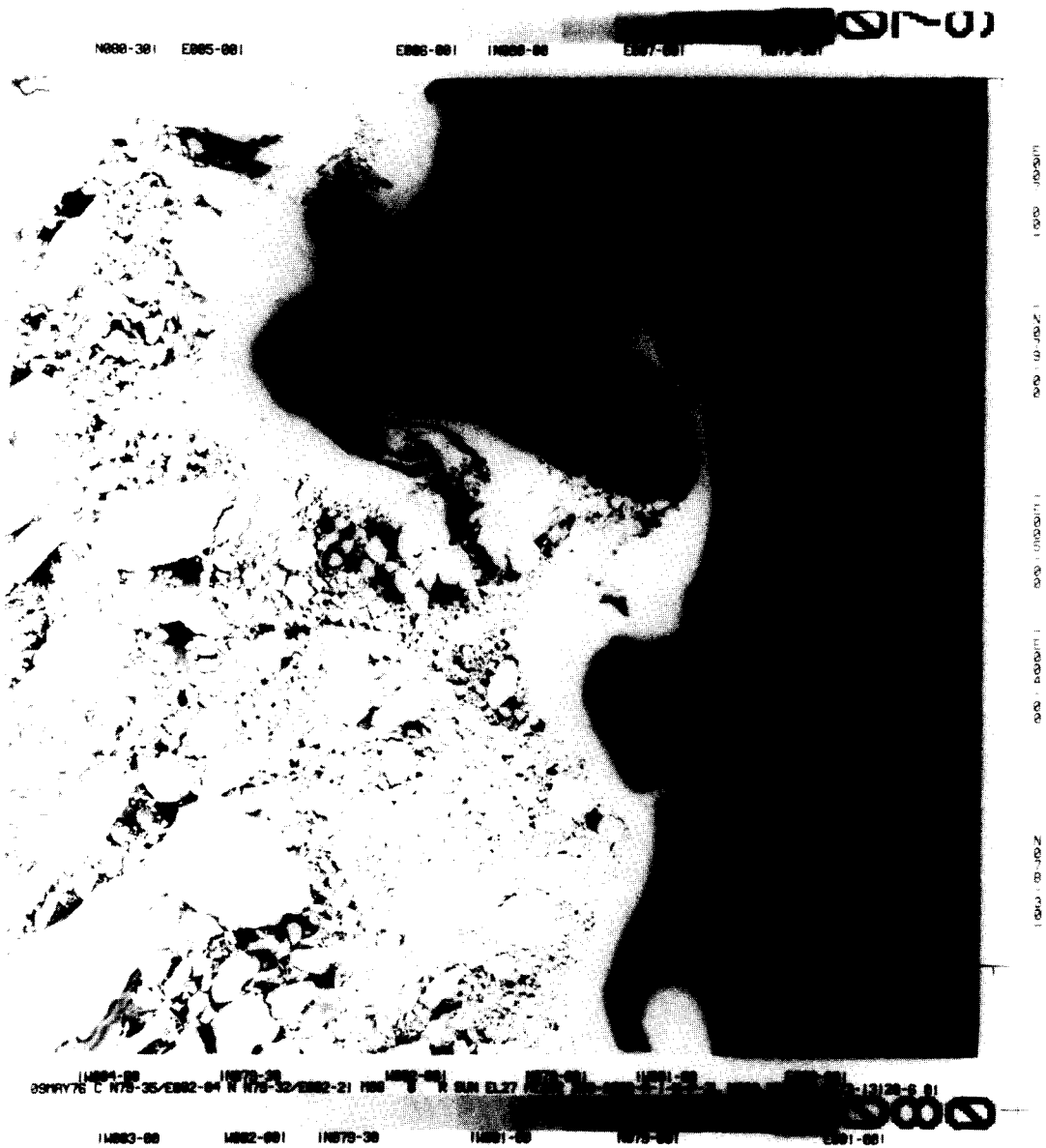


Fig. 12. Landsat image (MSS 6) obtained on 9 May 1976 showing an eddy at the ice margin. The centre of the eddy is at 79°30'N, 3°E. Geographical north is approximately 60° to the left of vertical. Image is 180 km square.

anecdotal material in SCORESBY (1820, Vol. 1, Ch. 4, Sect. VIII) to direct identification of an eddy by GLADFELTER (1964) and PALFREY (1967).

The feature in Fig. 12 appears very similar to surface eddies along the edge of the Labrador Current revealed by thermal infrared imagery (LEGECKIS, 1978). It is tempting to identify this eddy with the feature seen most clearly in Fig. 5, which covers exactly the same latitude range ( $80^{\circ}13'N$  to  $78^{\circ}52'N$ ) but is 50 km to the west ( $0^{\circ}W$ ). Whether this is really the same eddy, see three months after the data buoy entrapment, or whether the Front at this latitude is simply a fertile generator of eddies, is not clear. However the sound velocity profiles and the satellite images appear to be sensing an identical type of feature.

*Acknowledgements*—Our thanks are due to the captain and crew of HMS *Sovereign* for their skill and helpfulness in data collection throughout the cruise and to the Admiralty Research Laboratory, Teddington, for the velocimeter conversion and the installation of the Servoscribe recorder. One of us (PW) gratefully acknowledges the support of the U.S. Office of Naval Research, under contracts N00014-76-C-0660 and N00014-78-G-0003.

#### REFERENCES

- AAGAARD K. (1970) Wind-driven transports in the Greenland and Norwegian seas. *Deep-Sea Research*, **17**, 281–291.
- AAGAARD K. and L. K. COACHMAN (1968) The East Greenland Current north of Denmark Strait, Parts 1 and 2. *Arctic*, **21**, 181–200 and 267–290.
- BRITTER R. E. and J. E. SIMPSON (1978) Experiments on the dynamics of a gravity current head. *Journal of Fluid Mechanics*, **88**, 223–240.
- CSANADY G. T. (1972) Geostrophic drag, heat and mass transfer coefficients for the diabatic Ekman layer. *Journal of the Atmospheric Sciences*, **29**, 488–496.
- GILL A. E. (1973) Circulation and bottom water production in the Weddell Sea. *Deep-Sea Research*, **20**, 111–140.
- GLADFELTER W. H. (1964) Oceanography of the Greenland Sea, USS *Atka* (AGB-3) survey, summer 1962. Informal manuscript report 0-64-63, U.S. Naval Oceanographic Office, Washington D.C. 154 pp.
- JONES S. (1977) Instabilities and wave interactions in a rotating two-layer fluid. PhD Thesis, University of Cambridge. 295 pp.
- KILIERICH A. (1945) On the hydrography of the Greenland Sea. *Meddelelser om Grønland*, **144**, 63 pp.
- LEGECKIS R. (1978) A survey of worldwide sea surface temperature fronts detected by environment satellite. *Journal of Geophysical Research*, **83**, 4501–4522.
- LINDEN P. F. and J. E. WEBER (1977) The formation of layers in a double-diffusive system with a sloping boundary. *Journal of Fluid Mechanics*, **81**, 757–773.
- PALFREY K. M. (1967) Physical oceanography of the northern part of the Greenland Sea in summer 1964. Unpublished MS Thesis, University of Washington, Seattle. 52 pp.
- SAUNDERS P. M. (1973) The instability of a baroclinic vortex. *Journal of Physical Oceanography*, **3**, 61–65.
- SCORESBY W. (1820) *An account of the Arctic regions, with a history and description of the northern whale-fishery*. 2 Vols. Constable. Reprinted 1969, David & Charles Reprints, pp. 284–296.
- TOLSTOY I. and C. S. CLAY (1966) *Ocean acoustics*. McGraw-Hill, 293 pp.
- TURNER J. W. and C. F. CHEN (1974) Two-dimensional effects in double-diffusive convection. *Journal of Fluid Mechanics*, **38**, 375–400.
- VINJE T. E. (1977a) Sea ice conditions in the European sector of the marginal seas of the Arctic 1966–75. *Norsk Polarinstitutt Årbok*, **1975**, 163–174.
- VINJE T. E. (1977b) Sea ice studies in the Spitzbergen–Greenland area. Landsat Report E77-10206, US Department of Commerce, National Technical Information Service, Springfield, VA. 45 pp.
- VINJE T. E. (1979) On the ice transport between Greenland and Zemlja Franca Iosifa. To be published.
- WADHAMS P. (1977) A British submarine expedition to the North Pole, 1976. *Polar Record*, **18**, 487–491.
- WADHAMS P. (1978) Wave decay in the marginal ice zone measured from a submarine. *Deep-Sea Research*, **25**, 23–40.
- WADHAMS P. (1979) A comparison of sonar and laser profiles along corresponding tracks in the Arctic Ocean. *Symposium on Sea Ice Processes and Models*, Seattle, September 1977, R. A. PRITCHARD, editor, University of Washington Press. In press.